Renewable Diesel Boom and Market Transition Towards Resilience in Soybeans

Minseong Kang, and Seungki Lee

Suggested citation format:

Kang, M., and Lee, S. 2026. "Renewable Diesel Boom and Market Transition Towards Resilience in Soybeans." Proceedings of the NCCC-134 Conference on Applied Commodity Price Analysis, Forecasting, and Market Risk Management, Chicago, Illinois, April 20-21, 2026.
[http://www.farmdoc.illinois.edu/nccc134/paperarchive]

Renewable Diesel Boom and Market Transition Towards Resilience in Soybeans

Minseong Kang and Seungki Lee*

*** Preliminary and incomplete, please do not circulate. ***

Paper prepared for the NCCC-134 Conference on Applied Commodity Price Analysis, Forecasting, and Market Risk Management, 2026.

* Minseong Kang is a PhD candidate, and Seungki Lee is an Assistant Professor, both in the Department of Agricultural, Environmental, and Development Economics at The Ohio State University.

Renewable Diesel Boom and Market Transition Towards Resilience in Soybeans

Abstract: *The U.S. renewable diesel boom sharply expanded domestic soybean crushing, drawing a growing share of the crop into local processing and away from barge-borne exports down the Mississippi River. We ask whether this supply chain reorganization buffered inland soybean prices against river droughts. We estimate a storage-based structural VAR that allows crush activity to respond endogenously to market conditions, and identify river-disruption shocks using theory-based elasticity bounds. Holding crush activity at its pre-boom level, in the counterfactual analysis, reveals lower inland spot prices by 5.5 percent on average over 2021–2024. The resilience effect appears in spot prices and convenience yields, but not in futures prices, consistent with a local storage-demand channel. Our findings indicate that renewable diesel expansion changed not only the level of soybean demand, but also the price consequences of recurrent transportation shocks.*

Keywords: Renewable Diesel Boom, Mississippi River Drought, Competitive Storage Theory, Soybeans.

1. Introduction

Few developments have reshaped U.S. oilseed markets as quickly as the renewable diesel boom. Driven by federal tax credits, California's Low Carbon Fuel Standard, and a wave of refinery conversions, renewable diesel capacity expanded from roughly 1.6 billion gallons in 2021 to more than 5 billion in 2024, pulling a rising share of domestic soybean oil into the fuel complex (Gerveni et al., 2024; Troderman and Shi, 2023; U.S. EIA, 2024). The expansion did more than lift demand: it relocated where soybeans are processed and how they move. Crush capacity has multiplied across the Midwest (Gerlt, 2025), so a growing share of the crop is now processed locally and shipped as oil and meal by rail and truck, rather than moving as whole beans down the Mississippi to Gulf export terminals (CME Group, 2022; Denicoff et al., 2014). A supply chain that was historically barge-dependent and export-oriented has become more domestically oriented and geographically diversified. This shift has made local crush a more important outlet for soybeans, alongside the traditional river-to-Gulf export channel.

The existing literature frames biofuel demand primarily as a price-raising and volatility-amplifying force. For example, prior studies on the corn-ethanol expansion have established that mandated and subsidized biofuel demand pushes feedstock prices upward and tightens the link between energy and agricultural markets (Hertel and Beckman, 2011; Chen and Khanna, 2013; Zilberman et al., 2013; Roberts and Schlenker, 2013; Moschini et al., 2017; Lade et al., 2018). More recent contributions extend this logic to the renewable diesel era, treating the boom as a large positive demand shock to the soybean complex (Wu, Mallory, and Serra, 2025; Gerveni et al., 2024; Troderman and Shi, 2023). Across this literature, the central question is consistently how much biofuel demand raises prices. Important as that question is, it captures only the first-order price effect of biofuel demand and leaves open a different issue: whether the renewable diesel expansion also changed the soybean market's resilience.

This study asks whether the renewable diesel boom changed not only the level of soybean demand, but also the resilience of soybean prices to logistical disruption. Observed price changes during this period do not separately reveal that effect. Particularly, the observed boom that is pronounced since after 2021 coincided with an unusual sequence of large market shocks—the COVID-19 pandemic, the Russia–Ukraine war, and rapid growth in South American production—that shifted soybean demand, trade, and supply. Also, crush expansion itself is also an equilibrium response to expected returns, feedstock availability, and transportation access. Price changes during this period therefore confound the potential buffering effect of renewable-diesel-related crush expansion with other forces reshaping soybean markets. The empirical problem calls for a recurring downside shock that is central to soybean logistics but not itself a consequence of the renewable diesel boom.

We make use of Mississippi River droughts as a benchmark adverse shock to the soybean supply chain. These shocks are neither singular nor peripheral: they recur irregularly, and they strike a transportation artery that remains central to U.S. soybean exports. The Mississippi River system carries a substantial share of U.S. soybean exports, and recent droughts that lowered barge drafts and raised freight rates have been shown to depress prices near production regions and widen basis (Steinbach and Zhuang, 2025; Kang and Lee, 2025; Mitchell and Biram, 2025; Jo, Adjemian, and Mullen, 2025; Arita et al., 2022). Existing work therefore treats river drought as a price-moving logistical shock whose incidence falls on producers and shippers. Because the shock is recurring and tied directly to the river-to-Gulf export channel, it allows us to examine whether and to what extent expanded domestic crush has attenuated the transmission of river disruptions into local soybean prices.

Since the renewable diesel boom and river disruptions affect soybean prices through countervailing channels, we analyze them in a framework that also accounts for dynamic adjustment through storage and related market conditions. We therefore embed competitive storage model in a structural vector autoregression (SVAR), allowing prices, inventories, crushing demand, and transportation conditions to be jointly determined. This structure allows us to separate river disruptions from other shocks moving the soybean market while preserving the role of storage in price adjustment. Notably, storage is central in this setting: when transport bottlenecks strand beans inland, inventories rise and sales are deferred, smoothing the price response until conditions normalize (Working, 1949; Wright and Williams, 1982; Deaton and Laroque, 1992; Knittel and Pindyck, 2016).

Building on the storage-based SVAR of Carter, Rausser, and Smith (2017), we extend their framework in two ways. First, we model soybean crushing as an endogenous demand shifter with its own structural equation, rather than as an exogenous element of inventory supply, because crush capacity is jointly determined with prices. Second, because adding an endogenous crush equation breaks the monotonic mapping that point-identifies the four-variable model, we develop a set-identification strategy that combines theory-based elasticity bounds—derived from competitive storage theory and disciplined with external demand elasticities from Adjemian and Smith (2012) and Lusk (2022)—with a grid search over the admissible range of the inventory-supply elasticity (Carter, Rausser, and Smith, 2017; Kilian and Murphy, 2014). We then conduct two counterfactual experiments: the first replaces the structural inventory shock with a river-disruption index that captures only the barge-driven component (Kang and Lee, 2025), and the second additionally holds crush capacity at its pre-boom level, so that the gap between the two paths isolates the boom's buffering contribution.

We find that the renewable diesel boom effectively cushioned inland soybean prices against river disruptions. Absent the crush expansion, spot prices in the Iowa market would have been about 5.5 percent lower on average over 2021–2024 as a result of river shocks, with the buffering effect strongest at the height of the boom. The reorganization of the supply chain toward local processing and more flexible transport thus absorbed a substantial part of the price pressure that barge disruptions would otherwise have transmitted—evidence that the boom strengthened, rather than merely shifted, soybean-market resilience.

Our contribution is twofold. First, we provide the first evidence of a resilience benefit from biofuel expansion under logistical disruptions. By showing that biofuel-driven demand can indirectly shield commodity prices from logistical shocks, through local processing and route diversification, we bridge the biofuel-and-feedstock-price literature with research on agricultural transportation risk, two strands that have not previously been joined. Second, we introduce a set-identification approach for storage-based commodity price models that accommodates an endogenous demand shifter and isolates a logistical channel from concurrent shocks. The framework applies to other storable-commodity markets, offering a way to quantify how structural changes or policies buffer or amplify price effects amid overlapping disturbances, from geopolitical conflict to pandemics. As climate change raises the frequency and severity of disruptions to U.S. grain transportation, the findings also suggest that energy policy can reshape agricultural price dynamics through demand-side channels in ways that extend well beyond its intended scope.

2. Model

Our model adapts the storage-based structural framework of Carter, Rausser, and Smith (2017, hereafter CRS). CRS embed the competitive theory of storage in a structural VAR to ask how the expansion of corn-based ethanol reshaped the level and volatility of corn prices. Their central methodological move is to identify the structural shocks not by recursive timing assumptions but by bounds derived from storage theory on the short-run inventory-supply elasticity, which lets them separate storage demand from cash-market supply and demand within a single dynamic system. We adapt this framework to the soybean market to study a parallel question—how the renewable diesel boom reshaped soybean prices—and we adapt it in two specific ways. First, because the boom operates through soybean crushing, a price-responsive component of demand that is itself the object of study, we endogenize crush as a separate structural equation rather than leaving it inside an aggregate use shifter (developed below). Second, we use Mississippi River disruptions as the identifying logistical shock against which the boom's buffering role is measured. The remainder of this subsection lays out the mechanism, the equilibrium conditions we inherit from CRS, and the crush extension that distinguishes our specification.

2.1. Mechanism: Why Storage Dynamics Matter

A shock to a storable commodity is not merely a cash-market event. Because soybeans can be carried forward, storers internalize such shocks and reallocate them across time, so a disturbance in any single period is transmitted jointly through the physical inventory market and the market for storage services. Capturing the renewable diesel boom's buffering role therefore requires a dynamic structural framework rather than a static analysis of spot supply and demand.

Figure 1 illustrates the mechanism that motivates our model, building on the competitive storage tradition (Working, 1949; Wright and Williams, 1982; Carter, Rausser, and Smith, 2017). The two panels depict the markets the model links. In the upper panel, the inventory market, inventory supply is the soybeans left over after current use, while the downward-sloping inventory demand reflects how much the market chooses to carry forward: a high spot price makes selling now attractive and storing less so, whereas a low price rewards holding stocks in anticipation of higher future prices. The lower panel is the market for storage services. Once the equilibrium quantity to carry forward is determined above, that inventory must be physically stored, generating a derived demand for storage whose price, the expected appreciation defined as $E_t[P_{t+1}] - P_t$, is set against an upward-sloping storage supply.

Within this structure, river disruptions and the renewable diesel boom act as opposing forces. When barge navigation halts, soybeans accumulate locally and inventory supply shifts outward, moving the equilibrium from O to O', depressing spot prices and raising inventories, and raising storage prices. The crush expansion pulls in the opposite direction, absorbing the excess supply, drawing inventories down, lifting spot prices, and easing storage prices, so the equilibrium settles at O''. These adjustments propagate through inventory accumulation and release over time – the intertemporal transmission a structural storage framework is designed to capture.

2.2. Conceptual Framework

To capture this intertemporal mechanism occurring across cash and storage market, we outline a conceptual framework based on the competitive storage model, building on CRS.

In the cash market, the change in inventories equals production-side net supply minus current use, $\Delta N_t = Q^s(P_t, F_t, z_{1t}, \varepsilon_t^s) - Q^D(P_t, F_t, z_{2t}, \varepsilon_t^d)$, where P_t is the spot price, F_t the futures price, and z_{1t}, z_{2t} are exogenous supply and demand shifters. Inverting in the spot price yields the cash-market clearing condition

$$P_t = \mathcal{F}_s(\Delta N_t, F_t, z_{1t}, z_{2t}, z_{3t}, \varepsilon_{st}). \tag{1}$$

Because the structural innovations follow a first-order Markov process, the absence of arbitrage links the futures price to expected next-period stocks, $F_t = E_t[\mathcal{F}_s(.)]$, yielding the inverse inventory-demand schedule

$$F_t = \mathcal{F}_e(N_t, \varepsilon_{st}, \varepsilon_{et}, \varepsilon_{nt}). \tag{2}$$

The storage market, in turn, prices the service of holding stocks. Following Working (1949), the equilibrium price of storage is the marginal convenience yield ψ_t, governed by an inverse storage-demand schedule

$$\psi_t = \mathcal{F}_e(N_t, z_{3t}, \varepsilon_{nt}), \qquad \mathcal{F}_n' < 0, \tag{3}$$

so that convenience yield is high when stocks are scarce. The shifter z_{3t} explicitly admits transport conditions, since impaired barge navigation strands beans inland and raises the short-run value of holding local stocks. From the net cost-of-carry relationship, we work throughout with the cost-adjusted log spot price decomposed as $p_t = f_t + s_t$, where $f_t \equiv \ln F_t$ and $s_t \equiv \ln \psi_t$ is the log convenience yield (the spot-futures spread). This decomposition lets independent storage-demand shifts move s_t without being mechanically forced into f_t, which is central to the identification of our model.

In CRS, the entire current use Q^D enters the cash-market relation as a single aggregate, with demand shifts treated as exogenous disturbances to net supply. This is appropriate for their question, where aggregate demand is a well-behaved shifter and the composition of use is not itself the object of inquiry. Our setting differs on precisely this point. The disturbance we study, the renewable diesel boom, is not a shift in aggregate use but in one component of it: the demand for soybeans to be crushed for oil. Two features make the aggregation inadequate here. First, crush level is endogenous rather than exogenous: processing capacity expands in response to expected prices and crush margins, so folding it into an exogenous shifter or the inventory-supply residual would misattribute a price-responsive demand response to an exogenous source and contaminate the estimated elasticities. Second, the research question requires crush to be separable—to ask how much the boom buffered prices against river disruptions, we must be able to switch the crush expansion off in a counterfactual while leaving the rest of the equilibrium intact, which is possible only if crush carries its own structural equation and shock. We therefore depart from CRS by promoting crush from an implicit element of current use to an explicit endogenous variable. Decomposing current use into crush and non-crush components, $Q^u = Q^{crush} + Q^{other}$, inventory supply becomes

$$I^s = Q^s - Q^{crush} - Q^{other}, \tag{4}$$

and crush enters the VAR system as an additional equation alongside global activity, inventory supply, inventory demand, and storage demand.

2.3. Empirical Model

Log-linearizing the extended framework around the steady state, we collect the five endogenous variables in the state vector $X_t = (REA_t, c_t, i_t, f_t, s_t)'$, where REA_t is global real economic activity, c_t log soybean crush, i_t log inventory, and f_t, s_t the log futures price and log convenience yield. Augmenting the cash-market, inventory-demand, storage-demand, crush, and activity equations with a deterministic trend and quarterly dummies Z_t gives the structural form

$$AX_t = BX_{t-1} + \Gamma Z_t + U_t, \qquad E[U_t U_t'] = \Sigma, \tag{5}$$

where A is the contemporaneous coefficient matrix, U_t is a vector of mutually orthogonal structural innovations, and pre-multiplying by A^{-1} delivers the reduced-form VAR(1) we estimate. The structure of A – which entries are zero, which are sign-restricted, and which are tied together – is determined by the identification scheme set out next.

2.4. Identification

Restrictions. Based on the theory of competitive sotrage, three zero restrictions are imposed. Global economic activity does not respond at impact to U.S. soybean variables (four zeros in row 1); crush demand does not respond contemporaneously to futures-price or convenience yield shocks (zeros in row 2); and the supply of storage does not respond immediately to the futures price (zero in row 5). We further impose two sign restrictions to discipline the crush-inventory simultaneity: the contemporaneous response of crush demand to inventory is positive ($\alpha_{32} > 0$ in Equation (6)) and that of inventory to crush is negative ($\alpha_{23} < 0$ in Equation (6)). Finally, because agents respond to the spot price $p_t = f_t + s_t$ rather than to its components, the coefficients on f_t and s_t in the inventory-supply equation are restricted to be equally θ^s. Imposing these restrictions, the normalized contemporaneous matrix takes the form

$$A = \begin{bmatrix} 1 & 0 & 0 & 0 & 0 \\ -\alpha_{21} & 1 & -\alpha_{23} & 0 & 0 \\ -\alpha_{31} & -\alpha_{32} & 1 & -\theta^s & -\theta^s \\ -\alpha_{41} & -\alpha_{42} & -\alpha_{43} & 1 & -\alpha_{45} \\ -\alpha_{51} & -\alpha_{52} & -\alpha_{53} & 0 & 1 \end{bmatrix}. \tag{6}$$

Yet, the system is not point-identified, since the reduced form covariance matrix yields only 15 independent moments, one fewer than 16 free contemporaneous parameters (including 5 structural error terms) after imposing zero and equal-coefficients restrictions. We thus impose theory-based bounds to obtain admissible set for each structural unknowns (CRS, 2017; Kilian and Murphy, 2014).

Inventory-demand Elasticity. From the inventory-demand and storage equations, $f_t = \alpha_{41} REA_t + \alpha_{42} c_t + \alpha_{43} i_t + \alpha_{45} s_t + (lags)$ and $s_t = \alpha_{51} REA_t + \alpha_{52} c_t + \alpha_{53} i_t + (lags)$. Holding c_t fixed, $\partial s_t / \partial i_t = \alpha_{53}$ and $\partial f_t / \partial i_t = \alpha_{43} + \alpha_{45}\alpha_{53}$, so with $p_t = f_t + s_t$,

$$\frac{\partial p_t}{\partial i_t} = \alpha_{43} + \alpha_{53}(1 + \alpha_{45}) \qquad \Longrightarrow \qquad \theta^d \equiv \frac{\partial i_t}{\partial p_t} = \frac{1}{\alpha_{43} + \alpha_{53}(1 + \alpha_{45})}. \tag{7}$$

By the chain rule, the equal loading makes $\theta^s \equiv \partial i_t / \partial p_t$ the short-run elasticity of inventory supply with respect to the spot price. Because crush now enters as its own equation, this θ^s measures the response of stocks to price net of the indirect channel running through crush demand, an effect that is instead folded into the analogous coefficient of the four-variable CRS model.

Inventory-supply Elasticity. Differentiating (4) with respect to $\ln P$ and holding Q^{crush} fixed,

$$\theta^s \equiv \frac{\partial \ln I}{\partial \ln P}\bigg|_{crush\ fixed} = \eta^s \frac{Q^s}{I} - \eta^{other} \frac{Q^{other}}{I} \quad \Longrightarrow \quad \theta^s = -\eta^{other} \frac{Q^{other}}{I} \quad if \quad \eta^s \approx 0, \tag{8}$$

where η^s is the production elasticity and η^{other} the non-crush demand elasticity. Market clearing $Q^d = Q^{crush} + Q^{other} + I^d$ gives $\eta^d = \eta^{crush}\left(\frac{Q^{crush}}{Q^d}\right) + \eta^{oher}\left(\frac{Q^{other}}{Q^d}\right) + \theta^d\left(\frac{I}{Q^d}\right)$. Multiplying by Q^d/I and substituting into (8) yields the structural link between the two inventory elasticities,

$$\theta^s - \theta^d = \left(-\eta^d + \eta^{crush}\frac{Q^{crush}}{Q^d}\right)\frac{Q^d}{I}. \tag{9}$$

Point Estimate. Using sample averages, $\eta^d \approx -\frac{1}{1.12} = -0.893$ (Adjemian and Smith, 2012), $\eta^{crush} \approx -1.031$ (Lusk, 2022), crush share $Q^{crush}/Q^d = 0.517$, and $I/Q^d = 0.075$ from the USDA-ERS (2025) oil crops yearbook over 2007/08-2024/25, equation (9) gives $\theta^s - \theta^d = [(0 - (-0.893) + (-1.031 \times 0.517)]/0.075 \approx 4.80$, which together with (8) pins down the point estimate at the grid optimum.

Set Identification. Rather than rely on the point estimate alone, we bound θ^s. From (9) with $\eta^s \approx 0$, $\theta^s = |\eta^{other}|/(I/Q^{other})$, so the lower bound minimizes the numerator and maximizes the denominator. Adopting $|\eta^{other}| > 0.1$ and $I/Q^{other} \leq 0.497$ (the sample maximum – reached in 2018/19 when the U.S.-China dispute cut exports and raised ending stocks),

$$\theta^s_{min} = \frac{|\eta^{other}|_{min}}{\left(\frac{I}{Q^{other}}\right)_{max}} = \frac{0.1}{0.497} \approx 0.20. \tag{10}$$

The upper bound follows from the assumption that the elasticity of next period's net supply with respect to the expected future price is at least as large as that of current net supply with respect to the current spot price, which translates into $\theta^s \leq 1/|\alpha_{43}|$, where $\alpha_{43} = -\partial f_t/\partial i_t$ is estimated from the inventory-demand equation. The identified set is therefore

$$\theta^s \in \left[0.20, \frac{1}{\alpha_{43}}\right]. \tag{11}$$

Estimation proceeds by a grid search over this interval with step size 0.001: at each θ^s the remaining structural parameters are recovered by minimizing the distance between the model-implied and sample covariance matrices. Because the endogenous crush equation renders the mapping from θ^s to the structural parameters non-monotonic—unlike the monotone four-variable CRS model, whose identified set is characterized by its endpoints alone—the full grid is required. Inference uses a recursive-design wild bootstrap with 1,000 replications.

2.5. Estimation procedure

Estimation proceeds in three steps: reduced-form estimation, grid-based recovery of the structural parameters, and bootstrap inference.

Reduced form. We first estimate the reduced-form VAR(1),

$$X_t = \widehat{\Phi} X_{t-1} + \widehat{\Theta} Z_t + \hat{\varepsilon}_t, \qquad \widehat{\Sigma}_\varepsilon = \frac{1}{T}\sum_t \hat{\varepsilon}_t \hat{\varepsilon}_t', \tag{12}$$

on the full sample of $T = 71$ quarterly observations (2007Q1-2024Q4, after one observation is lost to the lag). Information criteria favor a single lag over two – AIC (-1600.4 vs -1561.6), AICc (-1591.3 vs -1532.0), and BIC (-1543.9 vs -1449.2) – consistent with CRS, so we estimate a VAR(1).

Structural recovery over the grid. The reduced-form innovations related to the orthogonal structural shocks through $\hat{\varepsilon} = A^{-1}U_t$, so that $\widehat{\Sigma}_\varepsilon = A^{-1}\Sigma_U (A^{-1})'$ with Σ_U diagonal. Because the system is only set-identified, we fix the inventory-supply elasticity at each point of a grid over the identified set $\theta^s \in [0.20, 1/\alpha_{43}]$ with step size $\Delta\theta^s = 0.001$, and at each grid point recover the remaining structural parameters $\Theta(\theta^s) = \{\alpha_{ij}, \sigma_k^2\}$ by minimum-distance estimation – minimizing the discrepancy between the model-implied and sample reduced-form covariances subject to the zero, sign, and equal-coefficient restrictions:

$$\widehat{\Theta}(\theta^s) = \text{argmin}_\Theta \left\| vech\left(\widehat{\Sigma}_\varepsilon\right) - vech\ \left(A(\theta^s)^{-1}\, \Sigma_U\, A(\theta^s)^{-1\prime}\right) \right\|, \tag{13}$$

retaining only parameterizations that satisfy $\alpha_{23} < 0$ and $\alpha_{32} > 0$. Unlike the four-variable CRS model, where the mapping from θ^s to the structural parameters is monotone and the identified set is pinned down by its two endpoints, the endogenous crush equation makes this mapping non-monotonic, so the full grid must be evaluated. The collection of admissible solutions $\{\hat{A}(\theta^s)\}_{\theta^s}$ traces the identified set for every structural object—the A matrix, the impulse responses, and the counterfactual paths.

Inference. Confidence bands are constructed by a recursive-design wild bootstrap. For each of $B = 1{,}000$ replications, we resample residuals with Rademacher weights, regenerate $\mathrm{X}_t^{(b)}$ recursively from (12) using the estimated reduced-form coefficients, re-estimate the reduced form, and repeat the grid-based recovery (13). Reporting the pointwise quantiles of the resulting distribution across replications—and, at each horizon, the union over the grid—yields bands that reflect both sampling uncertainty and the width of the identified set.

2.6. Counterfactual Design

Let $\hat{A}$, $\hat{B}$, $\hat{\Gamma}$ denote the estimated structural matrices and $\hat{U}_t$ the estimated structural shocks. The baseline trajectory reproduces the observed path by feeding $\hat{U}_t$ via the reduced form,

$$\hat{X}_t = \hat{A}^{-1}\hat{B}\hat{X}_{t-1} + \hat{A}^{-1}\hat{\Gamma}Z_t + \hat{A}^{-1}\hat{U}_t, \qquad \hat{p}_t = \hat{f}_t + \hat{s}_t, \tag{14}$$

where $\hat{X}_t = (REA_t, c_t, i_t, f_t, s_t)'$ and the log spot price is recovered from the futures-convenience yield decomposition.

Experiment 1 (CF1): River-driven disruptions only. We first isolate the river component of the inventory-supply shock by regressing the estimated shock on the Mississippi River disruption index as:

$$\hat{u}_{3t} = \alpha + \beta(River)_t + e_t, \tag{15}$$

and replace the third element of the shock vector with its fitted value $\hat{\beta}(River)_t$, leaving all other shocks at their estimates:

$$\widetilde{U}_t^{CF_1} = (\hat{u}_{1t}, \hat{u}_{2t}, \hat{\beta}(River)_t, \hat{u}_{4t}, \hat{u}_{5t})', \tag{16}$$

The CF1 path then follows the same recursion driven by this modified shock vector,

$$\tilde{X}_t^{CF_1} = \hat{A}^{-1}\hat{B}\tilde{X}_{t-1}^{CF_1} + \hat{A}^{-1}\hat{\Gamma}Z_t + \hat{A}^{-1}\tilde{U}_t^{CF1}, \qquad \tilde{p}_t^{CF1} = \tilde{f}_t^{CF1} + \tilde{s}_t^{CF1}. \tag{17}$$

Experiment 2 (CF2): river disruptions without the renewable diesel boom. Layering onto CF1, we switch off the crush shock from 2021Q1 onward, holding crush at its pre-2021 quarterly average level, by defining

$$\delta_{2t} = \begin{cases} \hat{u}_{2t}, & t < 2021Q1 \\ 0, & t \geq 2021Q1 \end{cases}, \tag{18}$$

so that the CF2 shock vector replaces both the crush and the inventory-supply elements,

$$\tilde{U}_t^{CF_2} = (\hat{u}_{1t}, \delta_{2t}, \hat{\beta}(River)_t, \hat{u}_{4t}, \hat{u}_{5t})', \tag{19}$$

and the CF2 path is

$$\tilde{X}_t^{CF_2} = \hat{A}^{-1}\hat{B}\tilde{X}_{t-1}^{CF_2} + \hat{A}^{-1}\hat{\Gamma}Z_t + \hat{A}^{-1}\tilde{U}_t^{CF2}, \qquad \tilde{p}_t^{CF2} = \tilde{f}_t^{CF2} + \tilde{s}_t^{CF2}. \tag{20}$$

Buffering measure. The two paths coincide through 2020Q4 and diverge once the crush shocks are muted from 2021Q1, so the percentage gap between them isolates the crush expansion's contribution to cushioning prices against river disruptions, net of the boom's direct demand-raising effect:

$$G_t = \frac{\tilde{p}_t^{CF2} - \tilde{p}_t^{CF1}}{\tilde{p}_t^{CF1}}. \tag{21}$$

3. Data

3.1. Construction of key variables

We use a quarterly panel of the Iowa soybean market spanning 2007Q1 to 2024Q4, yielding 72 observations (71 after one is lost to the lag). Iowa serves as an optimal setting for this analysis, because it is the second-largest soybean-producing state, the leading soybean-crushing state, and has direct access to the Mississippi River system for grain shipping. Consequently, the state functions simultaneously as a hub for crush expansion and as a market highly exposed to river droughts. This joint exposure motivates our empirical strategy to isolate these two distinct forces.

The model comprises five endogenous variables from the following sources. Global real economic activity is drawn from the Index of Global Real Economic Activity of the Federal Reserve Bank of

Dallas (2025) to absorb worldwide macroeconomic conditions that drive commodity price fluctuations. Monthly U.S. soybean crush volumes are reported by the National Oilseed Processors Association (2025; hereafter NOPA), aggregated to a quarterly frequency. Quarterly U.S. soybean ending stocks sourced from the USDA National Agricultural Statisics Service (2025; hereafter USDA-NASS). Daily CBOT soybean futures come from Barchart CmdtyView (2026) and convenience yield are calculated based on the net cost-of-carry relationship.

To ensure the quarterly futures price accurately tracks the supply conditions most relevant to each segment of the marketing year, we reference two distinct delivery contracts. In the first quarter, we utilize the March contract, whose delivery window coincides with the South American harvest—a period when Brazilian and Argentine supplies dominate global soybean balances. In subsequent quarters, we reference the new-crop November contract, which prices the forthcoming U.S. harvest. Aligning the delivery term with the harvest that establishes the binding supply signal in each quarter ensures the futures price remains anchored to a consistent, economically meaningful reference rather than a mechanically rolling nearby contract. Furthermore, this alignment captures the shifting competition between U.S. and South American origins. This structural choice is critical to our mechanism: soybeans constitute a major U.S. agricultural export, and Mississippi River disruptions transmit to prices primarily through their impact on export shipments routed to the Gulf of Mexico. Accurately capturing how futures prices embed these export-market flows—and how they reallocate as barge logistics tighten and U.S. supply competes with Brazilian exports—is essential for identifying the river-disruption channel.

The convenience yield – the marginal benefit of holding physical soybeans rather than a futures position – is not directly observed and is recovered from the net cost-of-carry relationship, consistent with the decomposition, $p_t = f_t + s_t$ in Section 3.2. Let P_t denote the real Iowa cash price, F_t real futures price constructed above, and m the number of months from the observation to the referenced contract's delivery such that $m \in \{2,7,4,1\}$ for the first through fourth quarters, corresponding to the January–March and April/July/October–November horizons. The convenience yield, s_t, is thus defined by the spread,

$$s_t = \ln\left(P_t\left(1 + \frac{r_t}{12}m\right) + k_t m\right) - \ln F_t\,,$$

where P_t is the monthly average soybean spot prices obtained from Iowa Cash Corn and Soybean Prices compiled by Iowa State University Extension and Outreach (2026) based on the USDA-NASS statistics, r_t is the one-year Treasury constant-maturity rate from Federal Reserve Bank of St. Louis (2025b; hereafter FRED), prorated to the holding horizon. k_t represents the physical storage cost per bushel per month based on Iowa warehousing rates. Since soybean warehousing costs are not directly reported, we set the monthly storage cost $k_t = \$0.08$ per bushels, following the Iowa Farm Bureau Analysis in 2022 (Gerdts, 2022).

Two features of this construction are important. First, horizon consistency. Scaling both the interest and storage terms by the actual months-to-delivery, m, ensures the cost of carry is horizon-consistent with the futures contract referenced in each quarter. Consequently, s_t measures the true convenience yield rather than mechanical variations in contract maturity. Second, scarcity signal. By construction, s_t rises when full carrying costs render the cash price expensive relative to deferred futures; that is, when physical stocks are scarce and the marginal value of holding inventory is elevated. This is precisely the margin through which river disruptions operate. When impaired barge navigation strands soybeans inland and increases the short-run value of local stocks, it manifests as a movement in s_t, making the convenience yield the natural link of the inventory-storage markets in our model.

To capture the low-water events along the Mississippi River system, we construct a river disruption index based on daily water-level records. We build on the identification strategy of Kang and Lee (2025), who use actual river-level data to empirically capture the comprehensive disruption status specific to each river route, linking this variation to barge freight rates. We construct a similar index; however, because our analysis is tethered to prices at the Iowa soybean market level, our index does not vary by specific route. Instead, we compile daily gage-height records from January 2007 to December 2024 from the USGS (2025) and USACE (2025) for 33 river gages spanning from Lock and Dam 13 (Fulton, IL)—the northernmost port along the Iowa-Mississippi River border—down to the Port of New Orleans, Louisiana. **Appendix Figure S1** illustrates the location of the gages included in the analysis. Following Kang and Lee (2025), for each gage, we define a low-water threshold at the 10th percentile of its historical daily distribution. A gage is classified as disrupted if its water level falls below this threshold. We compute the daily share of disrupted gages and average these shares to create a monthly river disruption index ranging from 0 to 1, where higher values indicate more pervasive low-water conditions. By capturing these exogenous river-level shocks, we identify the resulting buffering effect within the domestic market.

3.2. Summary statistics

Table 1 presents summary statistics for the key variables. Several patterns align with the economics of storage. Soybean crush rises rapidly in the late 2010s, rising from 418 million bushels over 2007-2010 to 526 million bushels in 2021-2024, reflecting the onset of the renewable diesel boom. U.S. soybean stocks average 1.38 billion bushels over the full study period but decline markedly from 1.75 billion bushels in 2016-2020 to 1.50 billion bushels in 2021-2024, as the domestic crush sector contemporaneously consumes a larger share of the crop. The futures price traces a trajectory inversely related to inventories, consistent with the theory of storage: it peaks at $13.1 in 2011-2015, when stocks are tightest at 1.06 billion bushels, falls to $9.3 in 2016-2020, when stocks are most abundant, and recovers to $11.0 in 2021-2024. The convenience yield follows the same scarcity logic, turning negative (-0.015) in the high-inventory 2016-2020 period, and rising to 0.051 in 2021-2024, when tighter stocks elevate the marginal value of holding physical soybeans. Finally, the river disruption index averages 0.098 overall but rising sharply to 0.175 in 2021-2024, up from a low of 0.016 in 2016-2020, capturing the severe low-water episodes on the Mississippi in 2022-2023.

It is noteworthy that every variable except inventories moves in the same direction from 2016-2020 to 2021-2024. This confounding is the central identification challenge of our study. Futures prices and convenience yield rise alongside not only the crush expansion but also a sharp recovery in real economic activity. The descriptive statistics alone thus cannot attribute the increase in soybean prices to any single driver. This motivates the structural approach developed above to tease out the contribution of each factor to soybean prices.

Figure 2 provides suggestive evidence of the supply-chain reconfiguration underlying our proposed mechanism. The plotted lines represent the monthly volume of U.S. soybeans moving down-river by barge, as a share of that year's total U.S. soybean production (by weight), before and after 2021.[1] The shaded areas illustrate the average monthly domestic crush level for each period. Domestic crush consistently sits above its pre-boom baseline throughout the calendar year, confirming the post-2021 expansion in soybean demand for biofuel production. The post-2021 trendline lies at or below the pre-2021 line in nearly all months except April, and this decline is heavily concentrated during the fall harvest peak when expanded domestic crushing competes most aggressively with export shipments for the newly harvested crop. At the annual level, the share of soybeans moved by barge falls from 11.3% to 9.8% in the post-boom period, supporting our reallocation hypothesis. Yet, the observed decline in the post-boom barge share may be confounded by the 2022–2023 low-water episodes. Isolating the effect of domestic reallocation from exogenous river disruptions requires the formal empirical approach outlined in the preceding paragraph.

4. Results

4.1. VAR Model Estimation Results

We estimate the reduced-form VAR(1) on the full sample of 71 observations from 2007Q2 to 2024Q4. **Table 2** reports the coefficient estimates, with each column corresponding to one equation of the system. The estimates show the persistence and cross-equation dynamics expected of a storage economy. All variables, except crush, are persistent in its own lag coefficients, with real economic activity (0.819) and futures price (0.853) showing particularly strong responses and inventories (0.480) and convenience yield (0.410) modest responses. Several lagged relationships accord with the theory of competitive storage. A higher lagged futures price predicts lower crush (-0.131), lower inventories (-0.842), and a higher subsequent convenience yield (0.133). When the deferred price is high, agents would draw down stocks, and the resulting scarcity raises the marginal value of holding inventory. Lagged crush is found to draw down inventories strongly (-1.909), reflecting

[1] Down-river soybean barge volume data, sourced from USDA-AMS (2025), is aggregated from weekly tonnage recorded at three lock sites, each located on one of the principal navigable rivers feeding the lower Mississippi: Lock 27 (near St. Louis, MO) on the upper Mississippi mainstream, above the confluence of the Mississippi and Ohio rivers at Cairo, IL; Lock and Dam 52 (near Paducah, KY) on the Ohio River; and Lock and Dam 1 (near Tichnor, AR) on the Arkansas River. Summing barge movements across these three points effectively captures soybeans flowing toward Gulf export terminals from the major tributary systems of the inland waterway network.

processing demand that competes for available stocks. Lagged real economic activity raises both crush (0.033) and inventories (0.190).

Turning to the estimates for the control variables, annual time trend is positive and significant for crush (0.015) and inventories (0.052) and mildly negative for the real futures price (-0.008), capturing the expansion of processing and stocks alongside a gentle decline in real prices over the sample. The quarterly dummies capture seasonality, particularly actively in crush and inventory demand equations, where the dummies for the first, second, and third quarter coefficients are large and negative relative to the fourth quarter (harvest) baseline.

4.2. Structural Estimates and the Identified Set

We recover the contemporaneous structural parameters by grid search over the admissible range of the inventory-supply elasticity, $\theta^s \in [0.20, 1/\alpha_{43}]$, with step size 0.001. The lower bound follows from the theory-based restrictions of **Section 2.4**, and the upper bound, determined endogenously by the estimated inventory-demand coefficient, evaluates to roughly 3.6, so the identified set is $\theta^s \in [0.20, 3.6]$ with a point estimate at the grid optimum of $\hat{\theta}^s \approx 2.44$. Across the entire grid, the structural estimates satisfy the imposed sign restrictions, and the model-implied covariance matrix closely matches its sample counterpart. **Table 3** reports the point estimates of the structural matrix A, with the identified set in brackets. **Appendix Figure S3** shows the grid search estimation results.

The key parameter, the contemporaneous response of inventory supply to the spot price, is estimated at $\hat{\theta}^s \approx 2.44$ and enters symmetrically on the futures price and the convenience yield through the equal-coefficient restriction, $p_t = f_t + s_t$. Its identified set, $[-3.60, -0.20]$ on each component, excludes zero, so the response is robust across the admissible range. The remaining contemporaneous elasticities are far more tightly identified. Crush demand responds negatively to inventory with a point estimate of -0.15 and a narrow set of $[-0.15, -0.14]$; inventory demand loads on the convenience yield with a coefficient near 1.12 ($[1.10, 1.13]$) and on inventory at 0.28 ($[0.18, 0.32]$); and the supply of storage rises with inventory at 0.08 ($[0.07, 0.08]$), consistent with the upward-sloping storage-supply schedule of the theory of storage. The narrowness of these brackets indicates that, even under set identification, the data pin down the rest of the contemporaneous structure with precision.

4.3. Impulse Response Function

Figure 3 plots the impulse responses to one-standard-deviation structural shocks over horizons 0 through 4 quarters. The shaded areas trace the identified set, and the vertical bars denote bootstrap confidence intervals with greater than 90% coverage, constructed from a recursive-design wild bootstrap with 1,000 replications. The responses are broadly consistent with the predictions of the competitive storage model, and the transmission of each shock works through inventory and storage dynamics rather than through prices alone.

The crush-demand shock is central to our mechanism. A positive shock produces a modest negative response of inventories at impact that becomes significantly negative in periods 1–2, as heightened processing draws down stocks before they gradually recover by period 4. Futures prices show a statistically significant, though small, positive response, indicating that crush expansion places mild upward pressure on price expectations. The convenience yield is insignificant on impact but turns significantly positive from period 1 onward, as the inventory drawdown raises the marginal value of holding stocks. That the convenience-yield response is delayed, mirroring the lagged inventory decline, confirms that the shock is transmitted through physical stock adjustment rather than immediate revaluation of expectations. Because the convenience yield reflects local market fundamentals, the pattern suggests that crush expansion not only lifts future price expectations but also tightens current fundamentals.

A positive inventory-supply shock raises crush demand, consistent with greater input availability supporting processing activity. It lowers futures prices from impact through period 4, with the effect fading gradually as the additional stocks ease scarcity, and it depresses the convenience yield—exactly the inverse inventory–convenience-yield relationship implied by the theory of storage.

The inventory-demand shock, which enters through the futures-price equation, raises inventories on impact: a higher expected return to carrying encourages speculative stock accumulation. From period 1 onward, inventories fall as those stocks are released back into the market. The convenience yield traces the opposite path, declining initially as inventories build and then rising as they are drawn down, again matching the inverse relationship between stocks and convenience yield.

Finally, a positive supply-of-storage shock, an increase in the convenience yield that signals greater current scarcity, generates a significant decline in futures prices. The market reads the scarcity as temporary: spot conditions tighten while futures fall as participants anticipate a supply recovery, thereby deepening backwardation. Taken together, the impulse responses confirm that the estimated system reproduces the inter-market dynamics consistent with the theory of competitive storage.

4.4. Counterfactual analysis.

We quantify the buffering effect of the renewable diesel boom with the two experiments. The first experiment isolates the river-driven path, while the second adds a "no boom" scenario after 2021 that holds crush records at its pre-2021 quarterly averages from 2021Q1. The changes in soybean spot prices under the second scenario compared to the first one measures how much lower prices would have been, under the same river disruptions, absent the crush expansion.

Figure 4 plots the percentage changes in each variable between two simulated paths. **Appendix Table S1** summarizes the annual average percentage changes in buffering effects. The results show that the renewable diesel boom has effectively cushioned soybean spot prices. Absent the crush expansion, inland spot prices would have been 5.5% lower on average over 2021–2024 because of river disruptions.

The other variables sharpen the mechanism. Without the boom, inventories would have been far larger, roughly 139% higher on average and up to 186% in 2024, because the absent crush demand would have left the soybeans that river disruptions stranded inland to accumulate as stocks. Futures prices, by contrast, are slightly increased by 2.9% on average, but the convenience yield show negative responses throughout the post-boom period. The results indicate that the boom firmed soybean spot prices relative to deferred prices, deepening backwardation. Taken together, the cushioning is a local storage-demand phenomenon rather than a revision of long-run fundamentals: by absorbing stranded beans into domestic processing in the near term, the boom strengthened local market fundamentals exactly when barge logistics tightened—the resilience channel the paper hypothesizes.

5. Conclusion

This paper investigates whether the renewable diesel boom buffered U.S. soybean prices against Mississippi River disruptions. By embedding competitive storage theory within a five-variable structural vector autoregression with endogenous soybean crush level, and identifying the river shock through a set-identification strategy combining theory-based elasticity bounds with a grid search, we find that the boom provided a substantial cushion to the market. Specifically, absent the crush expansion, inland spot prices would have been approximately 5.5% lower on average over 2021–2024 due to river shocks. This buffering effect is concentrated in the spot price and the convenience yield rather than the futures price, indicating that it operates through a local, physical storage-demand channel: by drawing stranded soybeans into domestic processing, the boom strengthened local market fundamentals precisely when barge logistics tightened.

Our study carry the first implication that biofuel policy can reshape agricultrual price dynamics through an unintended demand-side channel: by pulling feedstock into local processing, the renewable diesel boom quietly built resilience against logistical disruption that supply-focused assessments of biofuel mandates miss. Energy policy can thus reshape agricultural price risk through channels well beyond its intended scope. As climate change makes disruptions to U.S. grain transportation more frequent and severe, recognizing that where and how a crop is processed shapes its exposure to those shocks should inform both the management of agricultural price risk and energy policy.

Tables and Figures

Table 1. Summary Statistics

		Period			
Variable (unit)	Total	2007-10	2011-15	2016-2020	2021-24
Real economic activity	−0.015	0.870	−0.428	−0.412	0.112
Crush records (mil bu)	458.3	418.2	413.9	480.4	526.1
U.S. Soybean Stock (mil bu)	1377.7	1190.5	1061.7	1749.4	1495.3
Futures price ($/bu)	11.2	11.4	13.1	9.3	11.0
Convenience yield	0.015	−0.008	0.034	−0.015	0.051
River disruption index	0.098	0.058	0.149	0.016	0.175

Note: Columns report the full sample mean and four sub-period means. All price series are deflated using quarterly GDP deflator specific to the U.S. sourced from FRED (2025a).

Table 2. VAR (1) Parameter Estimates (N=71)

	Equations									
	REA_t		c_t		i_t		f_t		s_t	
Variable	Coef	SE	Coef	SE	Coef	SE	Coef	SE	Coef	SE
REA_{t-1}	0.819***	(0.07)	0.033***	(0.01)	0.109**	(0.04)	0.010	(0.02)	-0.012	(0.01)
c_{t-1}	0.035	(0.81)	0.193	(0.16)	-1.909***	(0.63)	0.062	(0.17)	0.170	(0.15)
i_{t-1}	0.125	(0.23)	0.007	(0.04)	0.480**	(0.23)	0.052	(0.05)	-0.022	(0.04)
f_{t-1}	-0.308	(0.31)	-0.131***	(0.04)	-0.842***	(0.20)	0.853***	(0.09)	0.133**	(0.05)
s_{t-1}	0.691	(0.92)	-0.001	(0.12)	-0.941**	(0.45)	0.254	(0.21)	0.410***	(0.13)
Year	-0.015	(0.02)	0.015***	(0.00)	0.052***	(0.01)	-0.008*	(0.00)	0.000	(0.00)
Q1	-0.558	(0.49)	-0.104	(0.08)	-1.474***	(0.52)	-0.021	(0.11)	0.017	(0.08)
Q2	0.010	(0.38)	-0.147**	(0.06)	-1.911***	(0.41)	-0.057	(0.08)	0.123**	(0.06)
Q3	-0.022	(0.27)	-0.186***	(0.05)	-2.809***	(0.30)	-0.014	(0.06)	0.068	(0.05)
Constant	30.576	(32.01)	-25.629***	(5.25)	-85.337***	(21.28)	15.824**	(7.24)	-2.164	(6.34)
R^2	0.756		0.862		0.947		0.754		0.487	

Notes: Rows are the variables included in each equation; columns denote the equations of the VAR system. Q1, Q2, and Q3 indicate dummy variable for the first, second, and third quarter, respectively. Year indicates yearly linear time trend variable. Robust standard errors are in parentheses. *, **, and *** indicate significance at the 10%, 5%, and 1% levels, respectively.

Table 3. Point Estimates and Identified Set A

Eqautions	Variables				
	REA_t	c_t	i_t	f_t	s_t
REA	1	0	0	0	0
Crush Demand	-0.03*** [-0.03, -0.03]	1	-0.15*** [-0.15, -0.14]	0	0
Inventory Supply	0.02 [-0.12, 0.09]	0.52*** [0.30, 0.70]	1	-2.44*** [-3.60, -0.20]	-2.44*** [-3.60, -0.20]
Inventory Demand	-0.10*** [-0.10, -0.09]	0.07*** [0.03, 0.09]	0.28*** [0.18, 0.32]	1	1.12*** [1.10, 1.13]
Storage Supply	0.03*** [0.02, 0.03]	0.05*** [0.04, 0.05]	0.08** [0.07, 0.08]	0	1

Notes: Rows denote the equations of the VAR system; columns denote the contemporaneous variable; and diagonal are normalized to one. For each cell, both point estimate and identified set based on grid search are reported. For the cells that are constrained to either 0 or 1, only the constrained values are reported. For point estimates, *, **, and *** indicate significance at the 10%, 5%, and 1% levels, respectively.

Figure 1. Illustration of the key mechanism

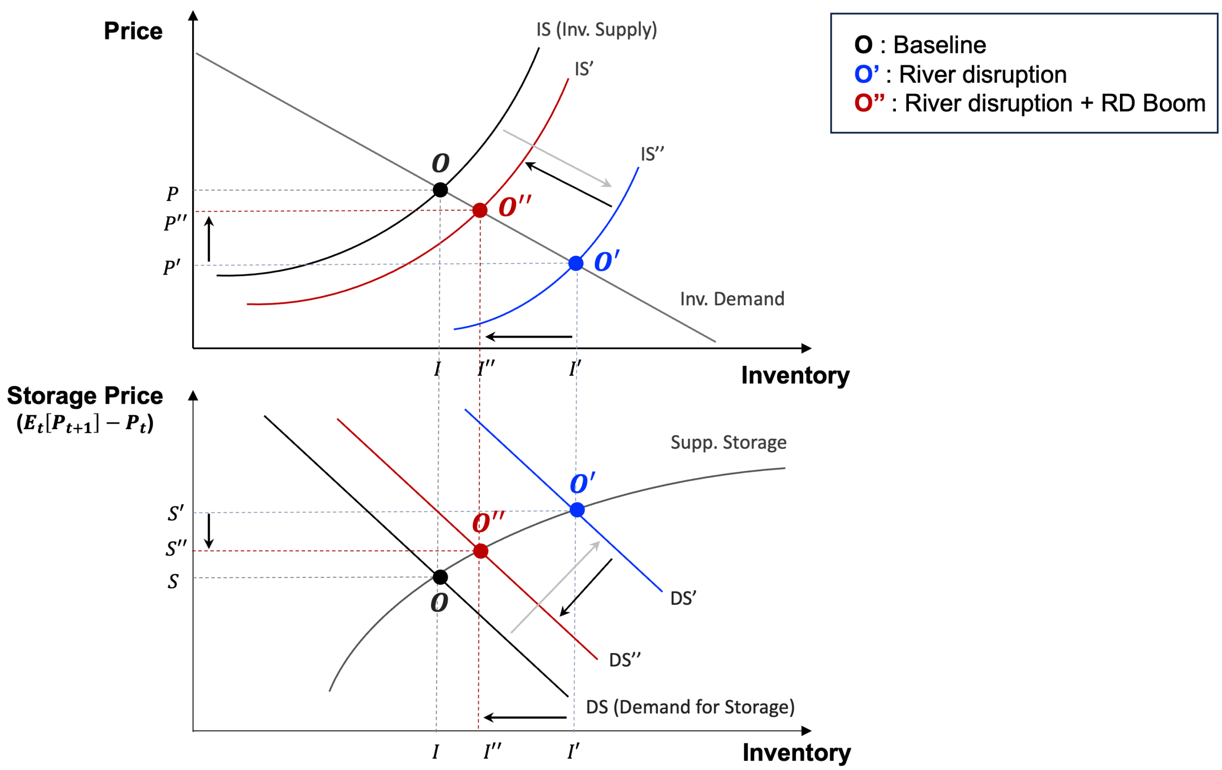

Figure 2. Evidence of the supply chain reconfiguration

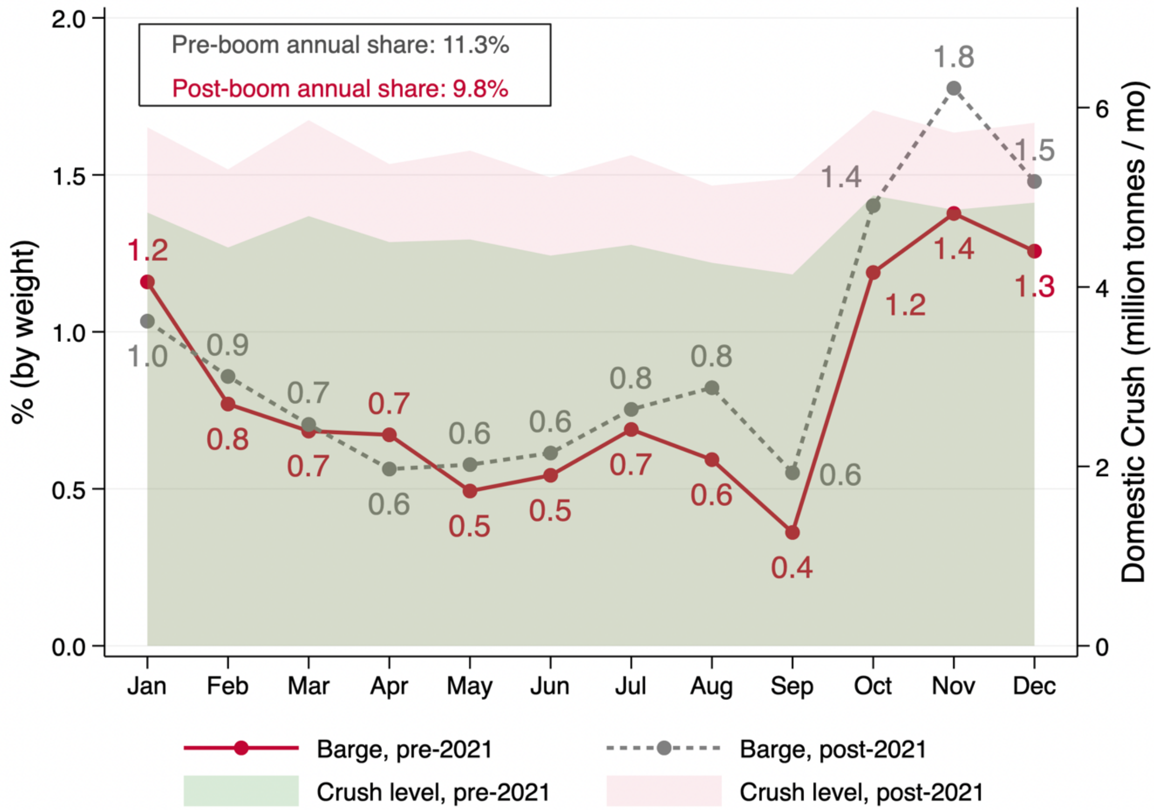

Note: Solid lines with markers indicate the average monthly share of soybean volumes moved downriver by barge relative to that year's total production, stratified by the periods before and after 2021. Aggregating these monthly figures across the calendar year reveals that the average annual barge share fell from 11.3% prior to the boom to 9.8% in the post-2021 period.
Source: NOPA (2025), USDA-AMS (2025), and USDA-NASS (2025).

Figure 3. Bootstrapped Impulse Response Function (1,000 Replications)

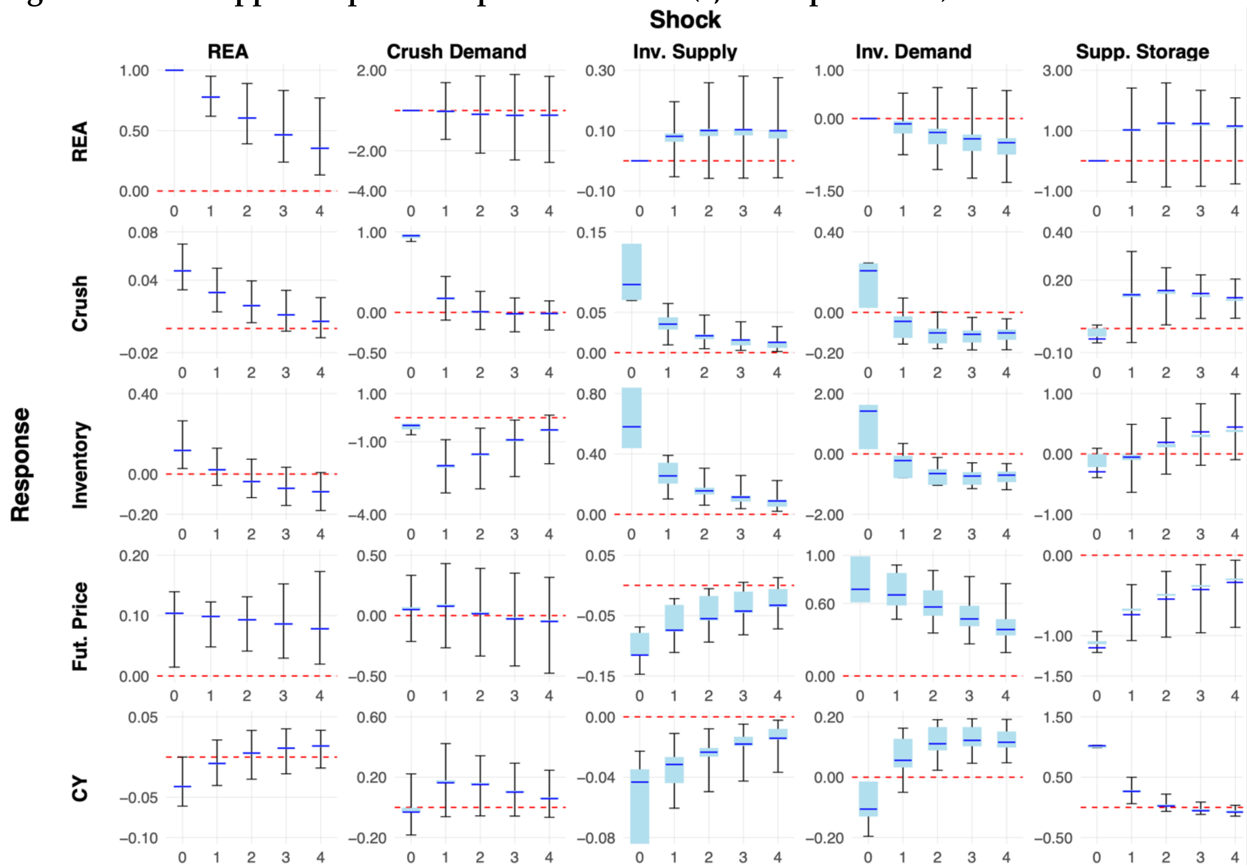

Notes: Each panel plots the impulse response of the row variable to a one-standard deviation structural shocks in the column variable over horizons of 0 to 4 quarters (x-axis). Blue horizontal dashes denote the point estimates at the grid optimum; light-blue shaded boxes trace the identified set across the admissible grid of the inventory-supply elasticity. Black vertical whiskers are bootstrap confidence intervals with greater than 90% coverage, constructed from a recursive-design wild bootstrap with 1,000 replications. The red dashed line marks zero.

References

Adjemian, M. K., and A. Smith. 2012. "Using USDA Forecasts to Estimate the Price Flexibility of Demand for Agricultural Commodities." *American Journal of Agricultural Economics* 94 (4): 978–995.

Arita, S., V. Breneman, S. Meyer and B. Rippey. 2022. "Low Mississippi River Barge Disruptions: Effects on Grain Barge Movement, Basis, and Fertilizer Prices." *farmdoc daily* (12):164, Department of Agricultural and Consumer Economics, University of Illinois at Urbana-Champaign.

Barchart CmdtyView. 2026. "CBOT Soybean Futures: Daily Settlement Prices." https://www.barchart.com.

Carter, C. A., G. C. Rausser, and A. Smith. 2017. "Commodity Storage and the Market Effects of Biofuel Policies." *American Journal of Agricultural Economics* 99 (4): 1027–1055.

Chen, X., and M. Khanna. 2013. "Food vs. Fuel: The Effect of Biofuel Policies." *American Journal of Agricultural Economics* 95 (2): 289–295.

CME Group. 2022. "Low Carbon Fuels Drive Vegetable Oil Price Volatility." October 14. https://www.cmegroup.com.

Deaton, A., and G. Laroque. 1992. "On the Behaviour of Commodity Prices." *Review of Economic Studies* 59 (1): 1–23.

Denicoff, M. R., M. Prater, and P. Bahizi. 2014. "Soybean Transportation Profile." Washington, DC: U.S. Department of Agriculture, Agricultural Marketing Service.

Federal Reserve Bank of Dallas. 2025. "Index of Global Real Economic Activity (IGREA)." https://www.dallasfed.org/research/igrea.

Federal Reserve Bank of St. Louis (FRED). 2025a. "Gross Domestic Product: Implicit Price Deflator (GDPDEF), 2017=100." https://fred.stlouisfed.org/series/GDPDEF.

Federal Reserve Bank of St. Louis (FRED). 2025b. "1-Year Treasury Constant Maturity Rate (DGS1)." https://fred.stlouisfed.org/series/DGS1.

Gerdts, A. 2022. "Soybean Storage, Will It Pay This Year?" Iowa Farm Bureau Federation, September 15. https://www.iowafarmbureau.com/Article/Soybean-Storage-Will-it-Pay-This-Year.

Gerlt, S. 2025. "Soybean Crush Expansion: 2025 Update." American Soybean Association. https://soygrowers.com.

Gerveni, M., T. Hubbs, S. Irwin, and S. Ramsey. 2024. "Updated Estimates of the Production Capacity of U.S. Renewable Diesel Plants Through 2026." *farmdoc daily* 14 (202).

Hertel, T. W., and J. Beckman. 2011. "Commodity Price Volatility in the Biofuel Era: An Examination of the Linkage Between Energy and Agricultural Markets." NBER Working Paper 16824. Cambridge, MA: National Bureau of Economic Research.

Iowa State University Extension and Outreach. 2025. "Iowa Cash Corn and Soybean Prices." Ag Decision Maker. https://www.extension.iastate.edu/agdm.

Jo, J., M. K. Adjemian, and J. Mullen. 2025. "How Much Do Transportation Backups Cost, and Who Pays for Them? The Case of the 2022 Mississippi River Backup." Working paper, University of Georgia.

Kang, M., and S. Lee. 2025. "Extreme Weather and Trade Costs: Evidence from Mississippi River Drought." SSRN Working Paper.

Kilian, L. 2009. "Not All Oil Price Shocks Are Alike: Disentangling Demand and Supply Shocks in the Crude Oil Market." *American Economic Review* 99 (3): 1053–1069.

Kilian, L., and D. P. Murphy. 2014. "The Role of Inventories and Speculative Trading in the Global Market for Crude Oil." *Journal of Applied Econometrics* 29 (3): 454–478.

Knittel, C. R., and R. S. Pindyck. 2016. "The Simple Economics of Commodity Price Speculation." *American Economic Journal: Macroeconomics* 8 (2): 85–110.

Lade, G. E., C.-Y. C. Lin Lawell, and A. Smith. 2018. "Policy Shocks and Market-Based Regulations: Evidence from the Renewable Fuel Standard." *American Journal of Agricultural Economics* 100 (3): 707–731.

Lusk, J. L. 2022. "Food and Fuel: Modeling Food System–Wide Impacts of an Increase in Demand for Soybean Oil." Report to the United Soybean Board. West Lafayette, IN: Purdue University.

Mitchell, J. L., and H. D. Biram. 2025. "The Effects of Extreme Weather on Rural Transportation Infrastructure and Crop Prices Along the Lower Mississippi River." *Applied Economic Perspectives and Policy* 47 (3): 1139–1161.

Moschini, G., H. Lapan, and H. Kim. 2017. "The Renewable Fuel Standard in Competitive Equilibrium: Market and Welfare Effects." *American Journal of Agricultural Economics* 99 (5): 1117–1142.

National Oilseed Processors Association (NOPA). 2025. "Monthly U.S. Soybean Crush." https://www.nopa.org.

Roberts, M. J., and W. Schlenker. 2013. "Identifying Supply and Demand Elasticities of Agricultural Commodities: Implications for the US Ethanol Mandate." *American Economic Review* 103 (6): 2265–2295.

Steinbach, S., and X. Zhuang. 2025. "US Agricultural Exports and the 2022 Mississippi River Drought." *Agribusiness* 41 (1): 289–303.

Troderman, J., and E. Shi. 2023. "Domestic Renewable Diesel Capacity Could More Than Double Through 2025." Today in Energy. Washington, DC: U.S. Energy Information Administration, February 2.

U.S. Army Corps of Engineers (USACE). 2025. "Water Levels of Rivers and Lakes (Rivergages)." https://rivergages.mvr.usace.army.mil.

U.S. Census Bureau. 2018. "Cartographic Boundary Files: States (cb_2018_us_state_500k)." https://www.census.gov/geographies/mapping-files.html.

U.S. Department of Agriculture, Agricultural Marketing Service (USDA-AMS). 2022. "Transportation of U.S. Grain: A Modal Share Analysis, 1978–2020 Update." Washington, DC: USDA-AMS.

U.S. Department of Agriculture, Agricultural Marketing Service (USDA-AMS). 2025. "Grain Transportation Report, Table 10." https://www.ams.usda.gov/services/transportation-analysis/gtr.

U.S. Department of Agriculture, Economic Research Service (USDA-ERS). 2025. "Oil Crops Yearbook." https://www.ers.usda.gov/data-products/oil-crops-yearbook.

U.S. Department of Agriculture, National Agricultural Statistics Service (USDA-NASS). 2025. "Quick Stats: Soybean Stocks, On-Farm and Off-Farm." https://quickstats.nass.usda.gov.

U.S. Department of Agriculture (USDA). 2025. "World Agricultural Supply and Demand Estimates (WASDE)." https://www.usda.gov/oce/commodity/wasde.

U.S. Energy Information Administration (EIA). 2024. "U.S. Biofuels Production Capacity Growth Slowed in 2024." Today in Energy. Washington, DC: U.S. Energy Information Administration.

U.S. Energy Information Administration (EIA). 2025. "Monthly Biofuels Capacity and Feedstocks Update." https://www.eia.gov/biofuels.

U.S. Environmental Protection Agency (EPA). 2025. "Renewable Fuel Standard Program: Annual Rules." https://www.epa.gov/renewable-fuel-standard-program.

U.S. Geological Survey (USGS). 2025. "National Water Information System (NWIS): Gage-Height Data." https://waterdata.usgs.gov/nwis.

Working, H. 1949. "The Theory of Price of Storage." *American Economic Review* 39 (6): 1254–1262.

Wright, B. D., and J. C. Williams. 1982. "The Economic Role of Commodity Storage." *Economic Journal* 92 (367): 596–614.

Wu, S., M. Mallory, and T. Serra. 2025. "Renewable Diesel Boom: The Impact of Soybean Crush Plants on Local Soybean Basis." Proceedings of the NCCC-134 Conference on Applied Commodity Price Analysis, Forecasting, and Market Risk Management, Chicago, IL.

Zilberman, D., G. Hochman, D. Rajagopal, S. Sexton, and G. Timilsina. 2013. "The Impact of Biofuels on Commodity Food Prices: Assessment of Findings." *American Journal of Agricultural Economics* 95 (2): 275–281.

Appendix Tables and Figures

Appendix Table S1. Counterfactual Analysis Results

		Years			
Variables	Total	2021	2022	2023	2024
Log Spot Price	-5.5%	-6.9%	-6.1%	-4.6%	-4.5%
Log Inventory	139%	94%	135%	149%	186%
Log Futures Price	2.9%	-0.7%	2.2%	4.3%	5.7%
Log Convenience Yield	-8.2%	-6.2%	-8.2%	-8.5%	-9.7%

Notes: The column 'total' reports average counterfactual changes under counterfactual scenario 2 compared to the first scenario for each variable after 2021Q1; the other year-specific columns annual average percentage changes in each variable under scenario 2 compared to the scenario 1.

Appendix Figure S1. Geographical location of the river level monitoring gages

Notes: The graph shows the geographical locations of the river-level monitoring gages included our analysis. The grey colored tringles indicate the river gages. Iowa, the geographic focus of our analysis, is shaded in red.
Source: USACE (2025) and USGS (2025).

Appendix Figure S2. Evolution of key variables over time

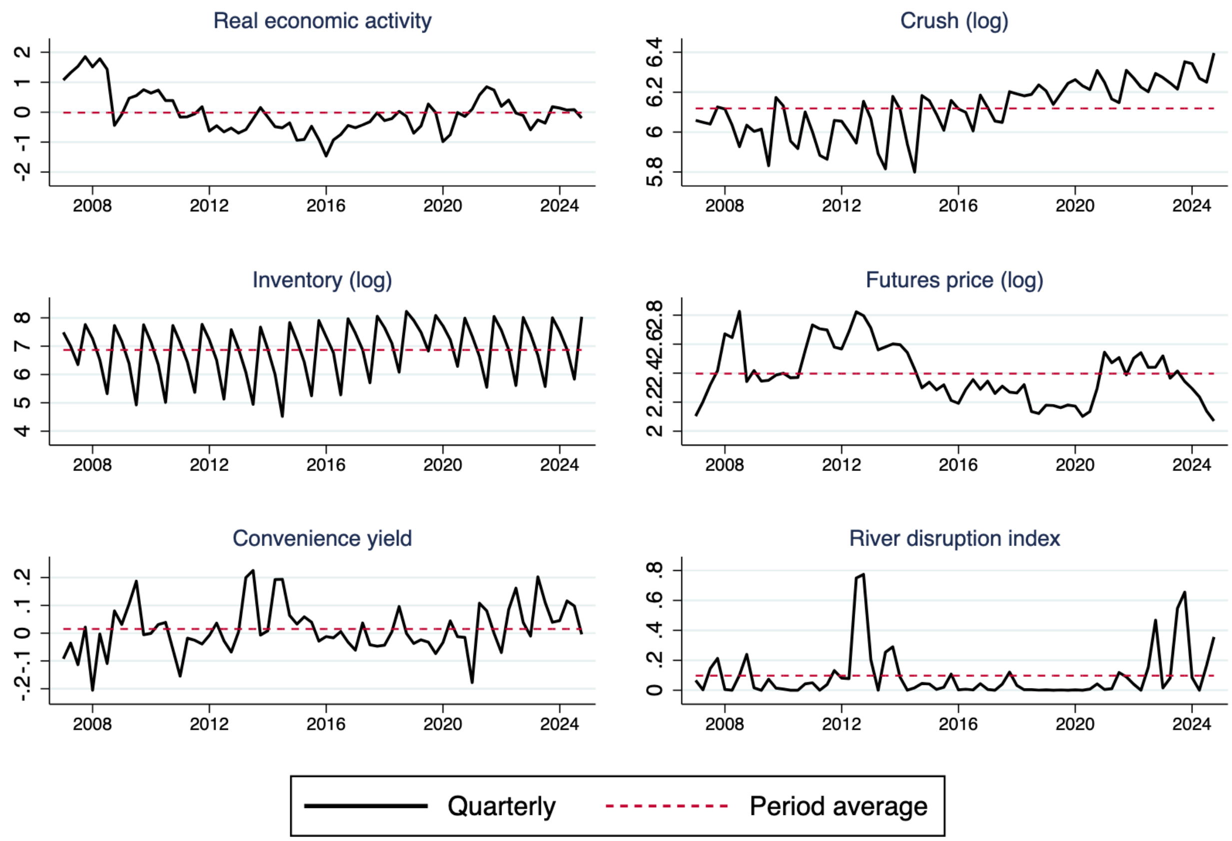

Notes: Each panel plots time trend of key variables used in the analysis, with crush level, inventory level, and futures prices recorded in log format.
Source: Federal Reserve Bank of Dallas (2025), NOPA (2025), USDA-NASS (2025), and Iowa Corn and Soybean Cash Prices (2026).

Appendix Figure S3. Identified Set of A Matrix

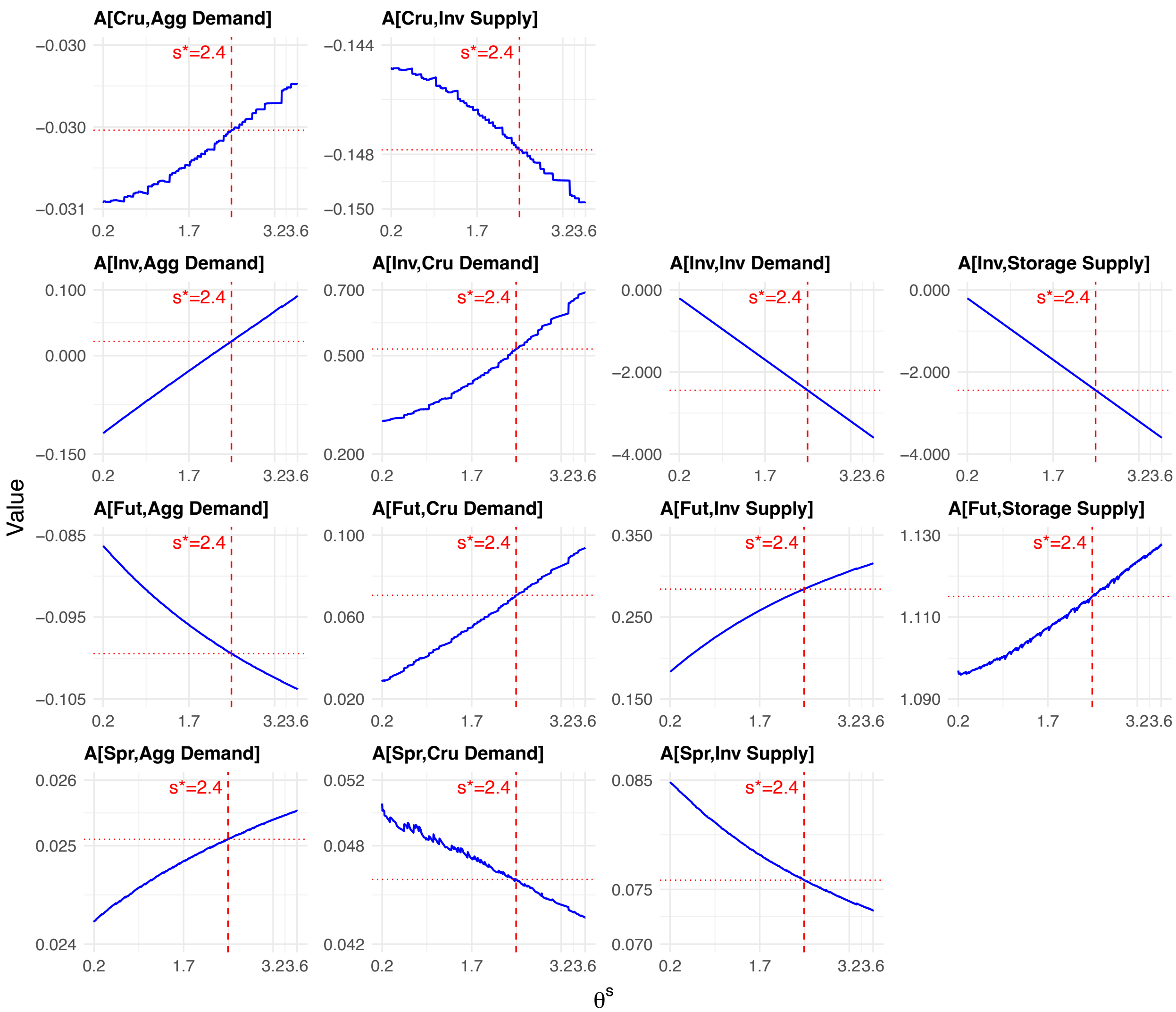

Notes: Each panel plots the identified set of set-identified parameters in structural matrix A. X-axis in all panels indicate the value of θ^s, and y-axis the corresponding value of each structural parameters. The red dashed line shows the point estimate threshold, $\theta^s = 2.4$.